IV International Conference on Particle-based Methods – Fundamentals and Applications
PARTICLES 2015
E. Oñate, M. Bischoff, D.R.J. Owen, P. Wriggers & T. Zohdi (Eds)

ADAPTIVE METHODS FOR THE SIMULATION OF MULTISCALE FLUID DYNAMIC PHENOMENA USING VORTEX PARTICLE METHODS WITH APPLICATIONS TO CIVIL STRUCTURES

DARIO MILANI[1], GUIDO MORGENTHAL[2]

[1] Bauhaus-Universität
99423, Germany
dario.milani@uni-weimar.de, http://www.uni-weimar.de/Bauing/MSK/19-en.html

[2] Bauhaus-Universität
99423, Germany
guido.morgenthal@uni-weimar.de, http://www.uni-weimar.de/Bauing/MSK/19-en.html

Key words: Adaptive Methods, Remeshing, Substepping, Vortex Particle Methods

Abstract. Wind effects on long-span bridges and slender buildings constitute a major criterion during the design phase. These effects are very important in certain cases, because they can lead to strong dynamic excitations of the structure and in some cases also to its failure. The shape optimazation often requires the usage of devices such as guide-vanes to enhance a passive flow control in order to reduce those excitations. Despite of their reduced dimensions, they often have a large influence on the entire flow field around the structure. It is then necessary to resolve the small scale fluid features that they generate. Vortex Particle Methods are successfully employed to study these phenomena. These methods consider a discrete number of mutual interacting vorticity-carrying particles to represent the continuous fluid domain. The boundary conditions are imposed by the Boundary Element Method approach which gives the advantage of a grid free Lagrangian formulation of the incompressible Navier-Stokes equations and a natural representation of the vortex creation process which is inherent in bluff body flows. This paper presents an adaptive scheme, the aim of which is the resolution of the small scale flow features in some regions by controlling the spatial and the temporal discretization of the problem of interest.

1 INTRODUCTION

A major criterion for designing civil structures is the estimation of the wind-induced response. Light flexible civil structures as long span suspended bridges are mainly bluff bodies. The wind caused forces lead in some cases towards strong excitation of the

structure and its failure. In these and many other cases it is very important to accurately resolve the flow field in order to evaluate the forces it provokes on the structure. The designer may choose to employ small-scale structures the aim of which is controlling the aerodynamic behaviour i.e. guide vanes in bridge design. In order to take into account their effect, the small scale features of the flow generated by these structured need to be accurately resolved. For these reasons it is required to resolve the multiscale phenomena on bluff bodies. The inherent unsteady flow field generated by bluff bodies is successfully resolved by Vortex Particle Methods (VPM). Furthermore the computational cost required to resolve the multiscale problem increases as the characteristic lengths difference. Adaptive methods needs to be employed in order to locally control the temporal and spacial discretization in order to resolve the smaller scales within certain regions e.g. around the guide vanes. In this paper a brief theory review of the general formulation of the Vortex Particle Methods (VPM) is firstly presented. Afterwards a description of the proposed adaptation schemes is detailed and an application of interest is presented.

2 THEORY REVIEW

A brief theory review is presented within the current section. The analytical expression of the Fluid Dynamic problem is derived, leading towards the formulation required for the Vortex Particle Methods (VPM). The equations are then discretized in order to enhance the numerical solution.

2.1 Analytical formulation

The aerodynamic problem satisfies in this framework the hypotheses of incompressibility of the fluid, zero summation of the external forces. When referring to an inertial frame the Navier-Stokes equations [1] are:

$$\frac{\partial \boldsymbol{u}}{\partial t} + (\boldsymbol{u}\nabla)\,\boldsymbol{u} = -\frac{1}{\rho}\nabla p + \nu\nabla^2\boldsymbol{u}, \tag{1}$$

$$\nabla \boldsymbol{u} = 0, \tag{2}$$

where ρ is the fluid density, $\boldsymbol{u}$ is the velocity vector, p is the pressure and ν is the kinematic viscosity. Vortex Particle Methods are successful techniques for modelling and simulating unsteady flow fields as in [7]-[9], require the vector vorticity $\boldsymbol{\omega}$ defined as:

$$\boldsymbol{\omega} = \nabla \times \boldsymbol{u}, \tag{3}$$

which appears by taking the curl of the Navier Stokes equations:

$$\frac{\partial \boldsymbol{\omega}}{\partial t} = \nabla \times (\boldsymbol{u} \times \boldsymbol{\omega}) + \nu\nabla^2\boldsymbol{\omega}, \tag{4}$$

$$\nabla \times \nabla \boldsymbol{u} = 0. \tag{5}$$

It is straightforward to observe that (5) is always satisfied while (4) can be furthermore simplified when the flow can be assumed as evolving in two dimensions:

$$\frac{\partial \omega}{\partial t} + (\boldsymbol{u} \cdot \nabla)\, \omega = \nu \nabla^2 \omega, \tag{6}$$

where the vorticity is a scalar field. When the fluid is also inviscid (6) reduces to:

$$\frac{\partial \omega}{\partial t} + (\boldsymbol{u} \cdot \nabla)\, \omega = 0, \tag{7}$$

or:

$$\frac{D\omega}{Dt} = 0, \tag{8}$$

which make use of the compact notation:

$$\frac{D}{Dt} = \frac{\partial}{\partial t} + (\boldsymbol{u} \cdot \nabla)\,. \tag{9}$$

The solution of the problem as expressed in (8) needs the velocity field to be computed and the boundary conditions to be applied. The boundary conditions are inherently applied using boundary elements. The velocity can be uniquely decomposed velocity into two different terms:

$$\boldsymbol{u} = \nabla \times \boldsymbol{\Psi} + \boldsymbol{u}_\infty, \tag{10}$$

where $\boldsymbol{u}_\infty$, is a constant describing the velocity at infinity and $\nabla \times \boldsymbol{\Psi}$ is the streamfunction. The curl of (10) leads to:

$$\nabla^2 \boldsymbol{\Psi} = -\boldsymbol{\omega}, \tag{11}$$

which is the Poisson equation associated to this problem. It is then possible to compute the streamline function $\boldsymbol{\Psi}$ through the usage of the Green's functions in two dimensions. By taking the curl of the computed $\boldsymbol{\Psi}$ the general expression of $\boldsymbol{u}$ is straightforward:

$$\boldsymbol{u}(\boldsymbol{x}) = \boldsymbol{u}_\infty - \frac{1}{2\pi} \int \int_D \frac{\omega(\boldsymbol{x}_0) \times (\boldsymbol{x}_0 - \boldsymbol{x})}{|\boldsymbol{x}_0 - \boldsymbol{x}|^2} dD_0. \tag{12}$$

With (12) it is possible to compute velocity field when the vorticity field is known.

2.2 Numerical discretization

The vorticity ω is constant along its streamline as (8) shows. The strategy adopted by the VPM consists then into the discretization of continuous vorticity and velocity fields into particles as in [5].The vorticity carrying particles evolve in a Lagrangian manner thus without the need for a grid. The discretization of the vorticity into N_p particles leads to the expression of the vorticity field as:

$$\omega(\boldsymbol{x}, t) = \sum_{p=1}^{N_p} \delta(\boldsymbol{x} - \boldsymbol{x}_p(t)) \Gamma_p, \tag{13}$$

where Γ_p is the particle's integral vorticity over it's surrounding area D_p:

$$\Gamma_p = \int_{Dp} \omega dD_p, \tag{14}$$

δ is the Dirac function, and $\boldsymbol{x}_p(t)$ is the particle location at a certain time t.
By combining (12) and (13) the vorticity field can be expressed as:

$$\boldsymbol{u}(\boldsymbol{x}_i, t) = \boldsymbol{U}_\infty - \sum_{p=1}^{N_f} \kappa \Gamma_p, \tag{15}$$

$$\kappa = \frac{\boldsymbol{e}_y \times (\boldsymbol{x}_i - \boldsymbol{x}_p)}{2\pi \mid \boldsymbol{x}_i - \boldsymbol{x}_p \mid^2}, \tag{16}$$

where e_y is the unit vector in the y direction perpendicular to the plane and κ is the velocity kernel. The velocity at any point is computed by summation of the contributions coming from the entire set of particles used to discrete the fluid domain. Afterwards $\boldsymbol{x}_p$ is computed by convecting the particles according to their velocities as:

$$\boldsymbol{x}_k^{n+1} = \boldsymbol{x}_k^n + \Delta t \boldsymbol{u}_k^n + O(\frac{1}{2}\Delta t^2 \boldsymbol{a}_k^n). \tag{17}$$

The computational cost CC required to solve the problems is dominated at each timestep by the (N_p^2) operations needed to resolve the mutual interaction among the N_p particles used to discrete the domain. This is necessary in order to compute each particle velocity as expressed in (15) at each timestep n. For a complete simulation the cost become:

$$CC = O(N_p^2 * N_t), \tag{18}$$

where N_t is the number of timesteps. If a body is immersed in the fluid domain, then its geometry also needs to be discretized. This discretization process is obtained by creating a polygon of N_i panels of lengths ds_i. At each panel central point the boundary conditions are enforced. This process leads towards a discretized representation of the the circulation on the surface γ_i defined over the panels. This circulation is then itegrated over each panel length and released onto the domain as circulation-carrying particles $\Gamma_i = \int_{ds_i} \gamma_i$. This procedure, namely Boundary Element Method, constitutes a major discussion within the advancement proposed in this paper. It has to be noticed that the computational cost needed to enforce the boundary conditions is smaller compared with (N_p^2) i.e. it is not taken into account.

3 ADVANCEMENT ON ADAPTIVITY

Equation (17) shows the importance of the choice of Δt namely temporal discretization, to predict the next position x_k^{n+1} prediction, while comparing (12) against (15) it is

possible to notice the importance of the spacial discretization to represent the whole flow field. Furthermore the Boundary Element Method implies that the particles are released from the surface at a certain timestep. The mechanism of particle releasing plays as well an important role when the performances are evaluated. The importance of these three aspects is at first individually pointed out as the improvements proposed.

3.1 Spacial adaptation

A spatial resolution improvement could be achieved by increasing N_p, but the computational cost would increase as N_p^2, as (18) shows. The strategy proposed allows to resolve the required features without increasing the total number of particles thus maintaining the computational cost. This will be achieved by modifying the particle map on the fluid domain using a grid. The VPMs are originally girdless methods because of the inherent Lagrangian formulation of the convection process as (8) exhibits. Recent advancements have been published which introduce a grid in order to accelerate the computation. An example are the Fast Multipole Methods [3] and the P3M algorithm [6]. The present method can be efficiently coupled with methods such as the [6] algorithm as a further extension. It is important to clarify that we refer to a mesh as to a collection of points on the fluid domain onto which the particles are projected thus constituting an updated set of particles. Within Fig. (1) the mesh is divided into two regions namely zones. On its right side the grid nodes spacing (δx) is equal to the one defined on the original uniform grid (Δx). We refer to this condition as 0 mesh *level*. On the left side of the grid it is possible to observe that $\delta x = 1/2\Delta x$. In this last case the mesh *level* is equal to one. The expression that links the local mesh $level = n$ and the local grid node spacing $(\delta x, \delta y)$ is:

$$(\delta x)_k = \frac{(\Delta x)_k}{2^n}, \qquad n \in \mathbb{N} \tag{19}$$

$$(\delta y)_k = \frac{(\Delta y)_k}{2^n}, \qquad n \in \mathbb{N} \tag{20}$$

where the new local mesh node spacing in a certain location k is $(\delta x)_k$ and $(\delta y)_k$. The *level* $n \in \mathbb{N}$ ensures the conformity of the adapted grid as it is shown in Fig. (1). The parameter n tunes the ratio of the initial x and y mesh node spacing to the adapted ones. According to (19) and (20), the particle spacing is reduced when n increases, and the particle density would be more important. It is then possible to compute a value of n which corresponds to the local need of spatial resolution within the same fluid domain to take into account the presence of the immersed bodies. The proposed expression for n is:

$$n_k(ds_j) = n_{panel}(ds_j) + a\|\mathbf{r}_{j,k}\| + b, \tag{21}$$

which is a linear expression in $\|\mathbf{r_{j,k}}\|$ whereas the coefficients a and b will be chosen to find an optimal balance between the accuracy requirements and the computational cost. The refinement factor computed for the particle k is $n_k(ds_j)$ where $\|\mathbf{r_{i,j}}\|$ is the distance to the

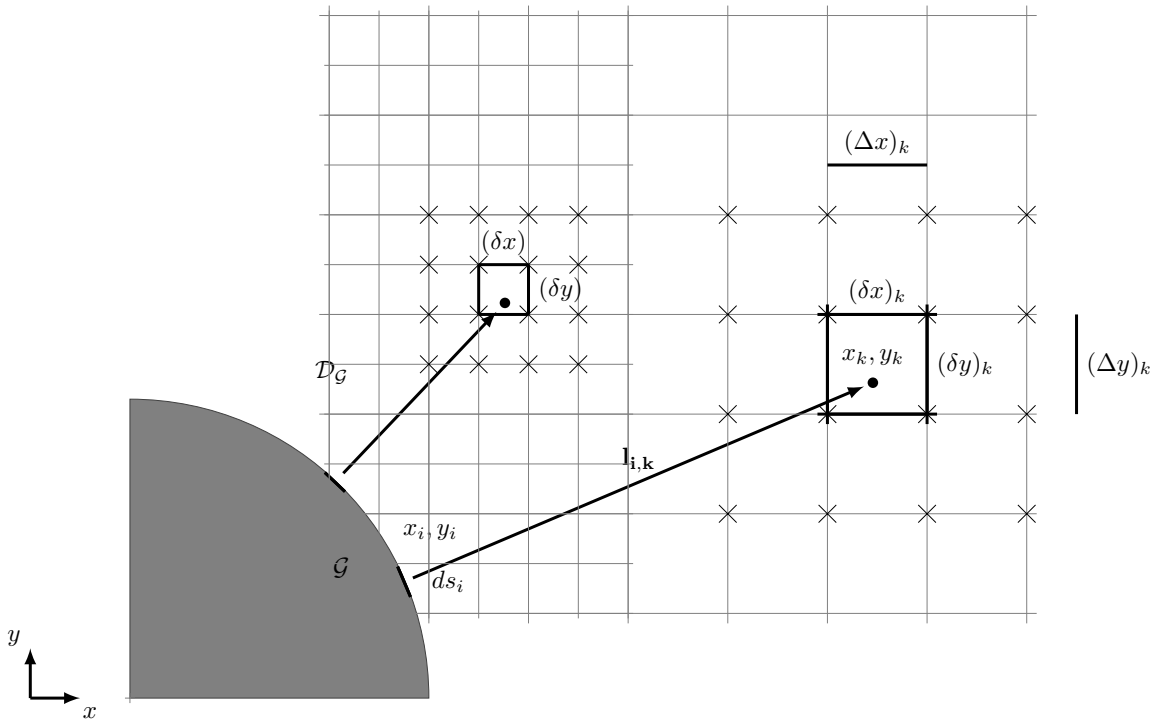

Figure 1: Remeshing strategy based on the distance to the closest surface panel i of length ds_i. The particle k located on the fluid domain at distance $\mathbf{l_{i,k}}$ to the closest panel has been projected on the surrounding mesh nodes. Another particle is located on the left side of the grid which is closer to the surface, thus has been projected on the surrounding refined mesh nodes.

closest panel j whose length is ds_j. It is possible to notice in Fig. (5) that the parameter a defines the distance to the surface at which n decreases. The parameter b sets an offset that can be chosen to increase the value of n for each particle. Finally $n_{panel}(ds_j)$ induces the parameter n_k to increase in those regions which are close to the small scale structures, such as the guide vanes. These structures are generally discretized with the finest set of panels in order to apply the boundary conditions, but also the surrounding regions need to be refined in order to accurately consider their influence over the entire problem. The refinement factor on the grid will then increase in order to generate the finest spatial resolution around those structures as:

$$n_{panel}(ds_i) = log_2(\frac{\sqrt{(\Delta x)^2 + (\Delta y)^2}}{ds_i}), \tag{22}$$

which can be reduced when dealing with homogeneous initial mesh ($\Delta x = \Delta y$) to:

$$n_{panel}(ds_i) = log_2(\frac{\Delta x}{ds_i}) \tag{23}$$

Equation (22) implies that an higher refinement factor is computed close to the smaller length panels. The real refinement factor applied should be an integer in order to assure the conformity of the adapted grid points. This is easily achieved by applying a rounding operator:

$$n_k = \max_i \left(n_k(ds_j) \right), \tag{24}$$

where the expression for $n_k(ds_j)$ was given in (21).

3.2 Temporal adaptation

Equation (17) shows how the temporal discretization affects the accuracy. Furthermore the example summarised in Figure (2) shows the impact of Δt on the resolution of a two interacting particles problem in which they are both assigned with a circulation of $\Gamma = 1\,[m^2/s]$. Their initial distance is $1\,[m]$ and they are free to convect. The circular pattern defines the analytical solution. After a period over T reach their initial position (thick line) while the discretized problem solved with (17) and (15) leads the particles distance to increase within the iteration process. The timestep adopted for the different

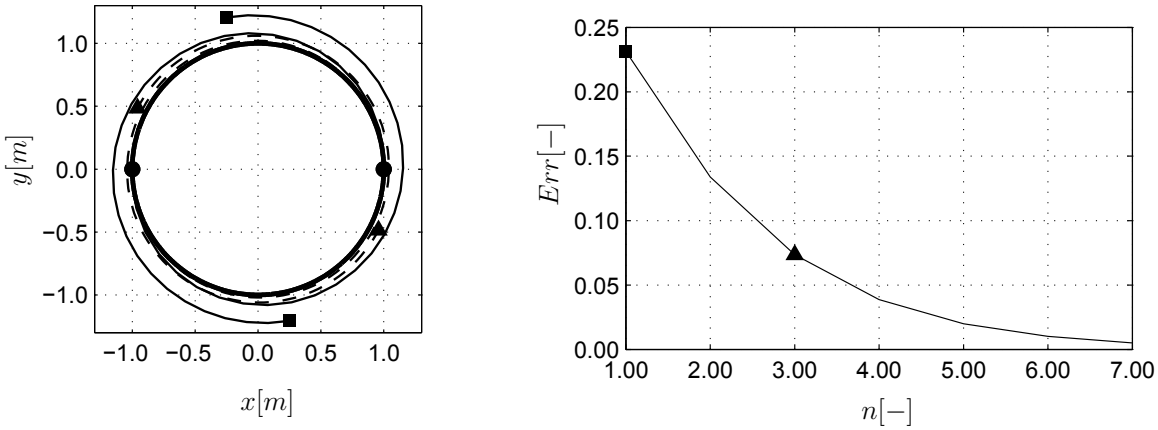

(a) Particle-Particle interaction path.

(b) Particle-Particle interaction error Err.

Figure 2: The round markers represent the initial position of the particles. The thick line represent the analytical solution of the problem requiring the particles to rotate and to reach their initial position over a period. The square and the triangle represent the final positions in (a) and the relative error in (b) when the substepping has been applied with different levels.

simulations is computed as:

$$\delta t = \frac{\delta t_0}{2^{level}}, \tag{25}$$

and the error Err is computed as:

$$Err = \frac{d - d_0}{d_0}, \tag{26}$$

where d_0 and d are respectively the initial and the final distance of the two particles and $\delta t_0 = T/60$. The analytical solution is characterised by $d = d_0$ that leads to $Err = 0$. It is then possible to increase the accuracy by reducing δt. The multi body problem represented by N_p particles is more difficult to solve and it does not have the analytical solution. However the considerations proposed for the two particles problem can be extended towards a complex case. The proposed strategy, proposes to classify the particles in different regions. Each one of those regions is assigned with a refinement factor n that determines the fractional duration of the local timestep duration to the global one. The particles belonging to regions in which n is large will convect with high accuracy because they velocities as in Fig. (3). Moreover the particles are introduced into the domain

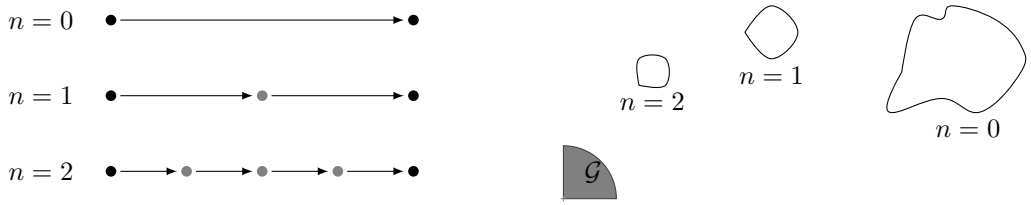

(a) Substep conformity (b) Substep regions

Figure 3: (a) The particles used to discretized the fluid domain are categorised in three regions based on their distance to the small structure $\mathcal{G}$. Each of these regions is assigned with a level n thus the local substep duration.(b).

through the external boundaries or they can be created on the surface of the immersed body thus released into the domain. For this second case a study has been performed in order to find the best way to couple the substepping strategy with the process of particle releasing. The first implementation of this strategy included the releasing of the particle at each timestep and substep. This procedure was improving the performance of the method although it was introducing numerical errors. A new procedure is presented within this paper in order to increase the impact of the strategy on the global performances. With that purpose the vorticity computed on the discretized surface is updated and released every timestep, as Fig. (4) shows, while only the iteration process occurs during the substeps. The computational cost is reduced because of the bound vorticity evaluations occurs once every timestep in spite of B times every timestep, where B is the number of timestep used to discretized the finest region, and a smaller amount of particles is released onto the fluid domain during a timestep. The accuracy increases because the boundary condition should be applied when the particles are coherently convected by the global timestep δt.

3.3 Full adaptivity

The substepping and the remeshing may be separately applied to the problem of interest. However it is important to notice that the spacial and the temporal discretization

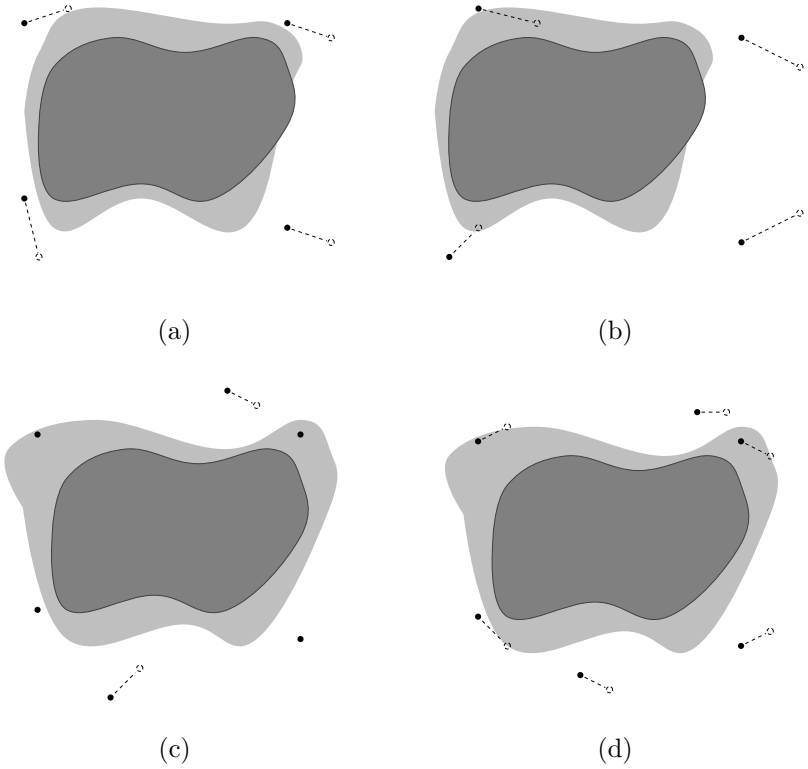

Figure 4: Releasing particle strategy from and immersed body; First substep $b = 1$ within a generic timestep s (a), particle convection process occurring from substep $b = 2$ until substep $b = B - 1$ (b), final convection substep $b = B$ within the timestep s with bound vorticity releasing into particles and computation of the new bound vorticity (c), convection of the new set of particles during the following timestep $s + 1$ (d).

are linked in all the numerical schemes present in literature e.g the Courant number [4] in finite difference schemes. Within this framework some numerical dissipation is introduced by the kernel in equation 16 because instabilities arise when the particle are close. When the remeshing and substepping strategy are applied together, the particle distance is controlled thus deleting the artificial dissipation.

With this purpose it is possible to compute a refinement factor n associated with the region of interest and to use simultaneously for the temporal and spacial discretization as prescribed. The next section will be devoted to apply these methods to a case of interest.

4 Reference object

The author chooses the Alcónetar Bridge as the reference object to exhibit the performances of these stategies. This bridge was built in 2006 in Spain in order to carry the route A-66 across the Tagus River. In spite of the low and regular speed of the air ($8m/s$), critical vibration episodes occurred. The introduction of the guide vanes allowed for a

passive control of the aerodynamic behaviour i.e. reducing the Vortex Induced Vibrations as in [8]. The two rectangular tandem arrangement that constitutes the shape of the bridge is shown in Fig. 5.

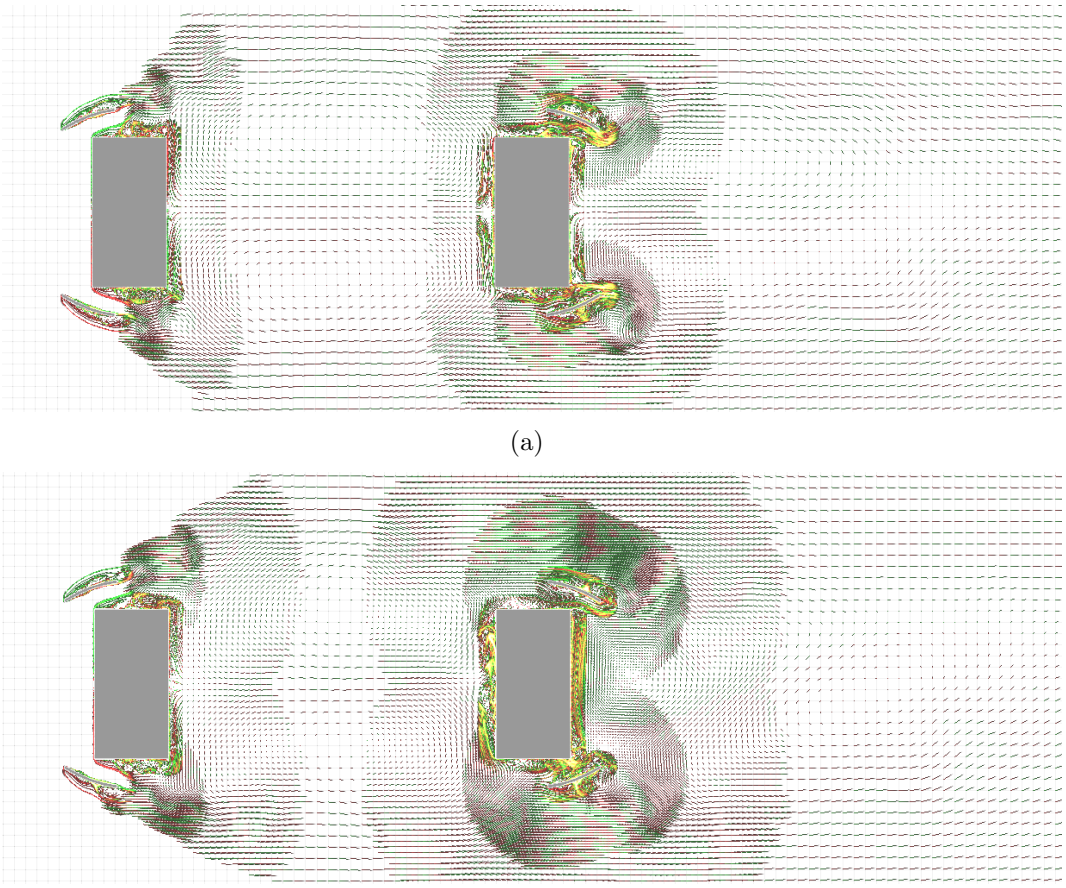

(a)

(b)

Figure 5: Projected particles for remeshing. In (a) the parameter $a1$ is equal to 1, while in (b) $a = 0.6$ in order to extend the high refinement region.

The guide vanes are used to reduce the Vortex Induced Vibrations (VIV). The herein proposed mesh adaptations schemes are applied in order to prove that it is possible to enhance a good accuracy by efficiently resolving the small scale flow featured around the guide vanes while saving computational effort.

4.1 Numerical results

The Vortex Particle Method solver used for implementation is VXflow [6]. The comparison has been performed in terms of Strouhal number:

$$St = \frac{f_S D}{U_\infty}, \tag{27}$$

where f_s is the vortex shedding frequency, D is the depth of the cross section and U_∞ is the wind speed. The aim of this comparison is to show that it is possible to largely reduce the computational cost (CC) with a moderate error (Err). The comprison is presented in Table 4.1. It is possible to confirm from previous studies, as in [8], that the Strouhal number value of this problem is around 2. The value that has been computed here stands in a very good accordance with the previous results: $St = 2.0439$ and it is taken as reference.

It is possible to define an averaged particles number $\bar{N}_{p_s}$ for each simulation s:

$$\bar{N}_{p_s} = \frac{\sum_{N_{t_s}} N_{p_s}(t)}{N_{t_s}}, \tag{28}$$

where $N_{p_s}(t)$ is the number of particles for each timestep t and N_{t_s} is the number of timesteps. The computational cost Cc_s already expressed in (18) is defined here with respect to a reference simulation $free$:

$$CC_s = \frac{(N_{p_s}^2 N_{t_s})}{(N_{p_{Free}}^2 N_{t_{Free}})}, \tag{29}$$

and the error Err is defined as:

$$Err_s(\%) = \frac{St_s - St_{Free}}{St_{Free}} * 100. \tag{30}$$

Table 1: Alcónetar bridge

	N_{p_s}	St_s	Cc_s	$Err_s(\%)$
Free	$3.7 * 10^5$	0.20439	1.00	0%
Remesh1	$8.1 * 10^4$	0.21855	0.05	5.81%
Remesh2	$1.1 * 10^5$	0.20752	0.09	1.52%
Remesh3*	$1.5 * 10^5$	0.20801	0.12	1.98%
Full adapt2	$2 * 2.1 * 10^5$	0.20308	0.33	−0.64%
Full adapt3*	$2 * 1.0 * 10^5$	0.20680	0.18	−0.71%

The results show that there is a satisfactory agreement with the literature St number and the simulations. In Ramesh1 Remesh2 and Remesh3 (Table 4.1) the refinement factor near the body surface increases. The accuracy increases coherently from Remesh1 to Remesh2. The accuracy lake in Remesh3 suggests that the particles distance in the close surface proximity is too small. In that case the substepping is needed in order to discard the artificial dissipation introduced by (16). Then the substepping is applied to this case in Full adapt3* improving the accuracy as expected. Another important remark

concerns the difference between the two particles releasing procedures which has already been explained. In Full adapt2 the particles are released at each timestep while in Full adapt3* they are released only once each timestep. The lack of accuracy within Full adapt3* is largely justified by the computational cost reduction due to the herein devised releasing process.

5 CONCLUSIONS

The computation of the Strouhal number is crucial in this framework as it allows to describe the behaviour of the bluff body problem. An accurate Strouhal number prediction means, for such a problem, that the small flow features are resolved using the herein proposed adaptive scheme. It is possible to conclude that the proposed strategy allows for the resolution of the small scales while maintaining an affordable computational cost.

REFERENCES

[1] A. Chorin, J. Marsden, *A mathematical introduction to fluid mechanics* volume 4. Springer, 1993.

[2] G. H. Cottet, P. D. Koumoutsakos, *Vortex methods: theory and practice*, 2001.

[3] Y. J. Liu, N. Nishimura *The fast multipole boundary element method for potential problems: a tutorial* Engineering Analysis with Boundary Elements 30.5 (2006): 371-381.

[4] R. Courant, K. Friedrichs, H. Lewy, *On the Partial Difference Equations of Mathematical Physics*, IBM J. 11, 215-234, 1967.

[5] J.H. Walther, A. Larsen, *Discrete vortex method for application to bluff body aerodynamics*, J. Wind Engineering and Industrial Aerodynamics, 67-68, 183-193, 1997.

[6] G. Morgenthal, *Aerodynamic Analysis of Structures Using High Resolution Vortex Particle Methods*, Ph.D. thesis, University of Cambridge, 2002.

[7] G. Morgenthal, A.S. Corriols, B. Bendig, *A GPU-accelerated Pseudo-3D Vortex Method for Aerodynamic Analysis*, Journal of Wind Engineering and Industrial Aerodynamics, 125 (2014), pp. 69-80, 2014.

[8] A.S. Corriols, G. Morgenthal, *Vortex-Induced Vibrations on Cross Sections in Tandem Arrangement*, Structural Engineering International (IABSE) 2013.

[9] J.M. Prendergast, *Simulation of unsteady 2-D wind by a vortex method*, PhD thesis, University of Cambridge, Department of Engineering, 2007.